1 Introduction

The first chapter is devoted to the traditional methods of fiber forming, which are used to produce macroscopic fibers. Since the novel methods used to form micro- and nanofibers described in this monograph have branched from the traditional methods, an introduction into the history of manmade fibers is instructive and fully appropriate (Section 1.1). There is a brief discussion of such traditional extrusion methods of fiber forming as melt spinning (Section 1.2), dry spinning (Section 1.3), wet spinning (Section 1.4) and the integrated process of spunbonding, which is used to form nonwoven fiber webs (Section 1.5). Melt and dry spinning are closely related to the electrospinning used to produce nanofibers, so the discussion of these traditional methods allows a first glimpse of electrospinning, covered in Chapter 5. One of the key elements of spunbonding is pulling polymer filaments by fast co-flowing air, which is known as meltblowing. Meltblowing, and its offshoot solution blowing, are also used to form micro- and nanofibers, as detailed in Chapter 4. In a sense, Section 1.5 serves as an introduction to the nonwoven nanofiber mats discussed later. Section 1.2 also contains some elements of quasi-one-dimensional theory; namely, its application to the draw resonance instability of melt spinning. In its more involved form a similar quasi-one-dimensional approach is applied in Chapters 3–6 to describe processes characteristic of melt- and solution blowing and electrospinning used to form micro- and nanofibers.

1.1 History and outlook

The term *fiber* originates from the French word *fibre*, from Latin *fibra* "a fiber, filament," of uncertain origin, perhaps related to Latin *filum* "thread," or from the root *findere* "to split" (Online Etimology Dictionary 2013). For centuries, the use of fibers was limited to natural materials such as cotton and linen, which had inherent problems with wrinkling. Silk was difficult to produce and was often too delicate. Wool was strong and abundant, but would shrink and was irritating next to the skin, and would not last long, as it was a food source for moths.

The idea of forming manmade fibers dates back to Robert Hooke and was expressed in 1664. In 1713, René Antoine de Réaumur produced the first spun glass fibers and in 1735 suggested forming fibers from liquid varnish. The initial progress paced in quanta of about 100 years, and in 1883 Sir Joseph Swan issued a solution of nitrocellulose in acetic

acid into a bath filled with alcohol, and thus realized the first wet spinning process, which formed long continuous fibers (Lewin 2007).

The invention of rayon extends back to 1855 in England, when Georges Audemars, a Swiss chemist, discovered how to make cellulose nitrate. In 1884 Count Hilaire de Chardonnet invented a method of forming fibers from regenerated cellulose. In 1889, the introduction of fabrics made of "artificial silk" at the Paris Exhibition received a lot of attention, and in 1891 Chardonnet established the first company in Besançon, France, producing the so-called Chardonnet silk fibers. After it was found that cellulose is soluble in aqueous solutions containing copper and ammonia, mass production of cuprammonium rayon fibers was started in Germany in 1899. The first rayon fiber was introduced as "artificial silk" partly because of its luster and its continuous filament nature. Viscose rayon fibers were introduced by Ch. F. Cross, E.J. Bevan and C. Beadle in 1893 and commercialized in England in 1905. The American Viscose Company, formed by S. Courtaulds and Co., Ltd, began production of rayon in 1910 in the USA.

The discovery of the origins of cellulose acetate is attributed to A.D. Little of Boston in 1893. Acetate was first introduced during 1904–1910, by two brothers, Camille and Henri Dreyfus in Basel, Switzerland (Morris 1989), making acetate motion picture film. The first commercial textile uses for acetate in fiber form are attributed to the Celanese Company in 1924. Manmade cellulosics are a major player in the fiber market today and are expected to continue due to their unique properties in terms of strength, flexibility and absorbency.

Nylon fibers were the first truly synthetic fibers that were industrially produced in 1939, thanks to the group led by W.H. Carothers. In 1931 Carothers reported on research at the DuPont Company on a polymer macromolecule called nylon 6,6. By 1938, P. Schlack of the I.G. Farben Company in Germany, polymerized caprolactam and created a different form of the polymer, identified simply as nylon 6. Nylon was the first commercially successful synthetic polymer. As the first synthetic fiber, nylon was designed to replace artificial silk. Nylon led to the global synthetic fiber revolution. Unlike rayon and acetate, which were derived from renewable cellulose stock, nylon was synthesized completely from petrochemicals. This first discovery led to the field of macromolecules and the new world of synthetic fibers. Nylon consists of repeating units linked by amide bonds and is frequently referred to as polyamide (PA). It is a thermoplastic, silky material, first used commercially in a nylon-bristled toothbrush (1938), and then for lady's stockings ("nylons"; 1940), after being introduced as a fabric at the 1939 New York World's Fair. Nylon stockings were shown in February 1939 at the San Francisco Exposition. The USA entered World War II in December 1941 and all production of nylon was dedicated for military use; nylon replaced silk in parachutes and flak vests, and found many other military uses.

That was the origin of all the modern manmade macroscopic synthetic fibers and modern textile industry. Polyester's commercialization in 1953 was accompanied by the introduction of triacetate. Today, polyester is the king of all synthetic fibers and is found in almost all apparel and many other applications. Polyesters have been developed with special shapes, fiber finishes, dyes and pigments, and consequently, offer the greatest level of control over the performance attributes important to the industries they serve.

The other important types of fibers and fiber products include *fiberboard*, made out of wood fibers (dating back to 1897), *fiberglass* (1937) and *fiber optics* (1956).

Today, fiber spinning is a commercial process to produce thin polymeric filaments that are used by a myriad of industries. Filaments can be produced from synthetic, manmade or natural polymers, usually by the process of extrusion. Extrusion is the process of forcing the raw materials in their liquid state through tiny orifices and solidifying them to form fibers. In their initial state the raw materials are solid. If they are thermoplastic polymers they are heated or melted, while if they are nonthermoplastic, they are dissolved in a suitable solvent. While we now take these processes for granted, it is interesting to note that their history only extends back about a century, and rayon was the first manmade fiber introduced only 160 years ago. Today, manmade fibers are found in almost every application, ranging from apparel and home furnishings, to automotive industry and medicine. The introduction of manmade and synthetic fibers has led to the introduction of many high-performance products touching many different industries. It is hard to imagine what we would have used for these applications today without access to these innovations.

The birth of nanofibers is related to the patent by Formhals (1934), in which electrospinning of cellulose acetate fibers was proposed. Electrically driven jets were in focus much earlier (Zeleny 1914, 1917); however, these were jets of inelastic Newtonian liquids, which are prone to capillary instability and cannot be used to form long cylindrical filaments. Only the presence of viscoelasticity in the solutions used by Formhals allowed him to form fibers. Moreover, these were nanofibers, since the presence of the electric forces results in dramatic reduction of the fiber cross-sectional diameter due to the so-called electrically driven bending instability found much later by Reneker *et al*. (2000). The nanoscale of the fibers was actually considered to be a drawback in the time of Formhals, since they could not be used in the textile industry. As a result, they did not stir up too much interest, and only occasional publications related to the electrically driven jets of polymer solutions and melts, and the fibers formed from them appeared in the 60 years after Fromhals' work (Baumgarten 1971, Larrondo and Manley 1981a, 1981b, 1981c). However, the situation had radically changed after the work of D.H. Reneker's group in the 1990s (Doshi and Reneker 1995, Reneker and Chun 1996). This was the time of nanotechnology, new applications of nanofibers were immediately recognized and the number of publications devoted to nanofiber forming started to increase exponentially. This process continues today and is described in the technical sections of this book.

The works on traditional and novel methods of fiber forming encompass synthetic chemistry, polymer physics, non-Newtonian fluid mechanics, electrohydrodynamics, applied mathematics and materials science, and require the concerted efforts of specialists from distant fields. The need for a comprehensive monograph encompassing different aspects of fiber-forming processes materialized first in the seminal monograph by Ziabicki (1976). With interest in nanofibers growing, several monographs exclusively devoted to electrospinning were published. Ramakrishna *et al*. (2005) covered the rapidly widening biomedical applications of electrospun nanofiber mats. Filatov *et al*. (2007) described the work of Petryanov-Sokolov's group in the Soviet

Union, which resulted in electrospun filters for protection from radioactive aerosols. Wendorff *et al*. (2012) discussed in depth the aspects of electrospinning related to materials science.

The existing and rapidly extending processes for forming micro- and nanofibers include meltblowing, electrospinning, solution blowing and several other methods. The fibers are formed from petroleum-derived and biopolymers. The scientific foundations of fiber-forming processes and their practical implementations are rooted in polymer physics, rheology, non-Newtonian fluid dynamics, electrohydrodynamics, aerodynamics and applied mathematics, while their applications extend to filters, membranes, electrodes, coatings, nanofluidics, communications (optical fibers), sensors, biomedical scaffolds and drug delivery, as well as various military-oriented aspects. The present monograph aims for a comprehensive in-depth description of all these aspects.

1.2 Melt spinning

The basic principle of fiber extrusion involves feeding pellets or granules of the solid polymer into an extruder. The pellets are compressed, heated and melted by an extrusion screw, then fed to a spinning pump and into the spinneret. The polymer is passed through the extruder and then a filter, to a manifold, and is distributed to one or more spinning positions (Hensen 1997).

The spinneret is the main component in determining fiber shape and size after extrusion. It may contain one to several hundreds of capillaries for filament spinning. In the case of spunbond systems, discussed in more detail in Section 1.5, there are as many as 6000 capillaries per meter. These tiny openings are very sensitive to impurities, damage and corrosion. When warranted, the spinneret can be made from very expensive, corrosion-resistant metals – for example, for extruding fluoropolymers such as perfluoroalkoxy polymer resin (PFA) and polyvinylidene difluoride (PVDF), as well as other exotic polymers such as polyphenylene sulfide (PPS). The polymer liquid feeding them must be carefully filtered, and should not leave residue on the face of the spinneret, as this would lead to breaks and drips. Most polymers have lubricants, anti-oxidants and other additives compounded into them to overcome challenges due to polymer degradation, and spinning breaks and drips. Maintenance is also critical, and spinnerets must be removed and cleaned on a regular basis to prevent clogging.

Thus, the term extrusion in the fiber industry refers to the process of forming polymeric filaments by forcing the fluid through a spinneret, and spinning is the collective term used for the extrusion and solidification of the filaments produced.

An important element is fiber drawing following the extrusion. Drawing results in the desired properties in the final product and in a decreased fiber diameter, increased molecular orientation, increased tensile properties and a reduction in strain to failure. The extent to which fibers can be drawn depends on the properties of the materials being extruded. Fibers are drawn as much as eight times their original length to form fibers with the desired properties.

It is interesting to note also that some polymers such as polyester (PET) require a high fiber spinning speed to form crystallinity. At about 3200 m min^{-1} PET starts to show signs of crystal orientation. Fibers spun at low speed shrink extensively if exposed to heat. For PET, therefore, fibers are extruded at much higher speeds – 4000 to 10 000 m min^{-1} – to overcome the issues with shrinkage.

There are several methods for forming fibers from molten state or from solution: melt, dry, wet and gel spinning. These are briefly described in this and the following sections. In melt spinning, the fiber-forming polymer is melted and extruded through the spinneret, stretched and directly solidified by cooling (Figure 1.1) and then drawn to achieve higher degrees of orientation and crystallization. Examples are polypropylene, polyester and nylon, among others. Melt spinning is by far the most widespread system globally. Continuous filaments, as well as discontinuous crimped fibers (also referred to as staple fibers), are globally available. The process for forming continuous filaments is somewhat different from those for producing staple fibers. Staple fibers are produced in continuous

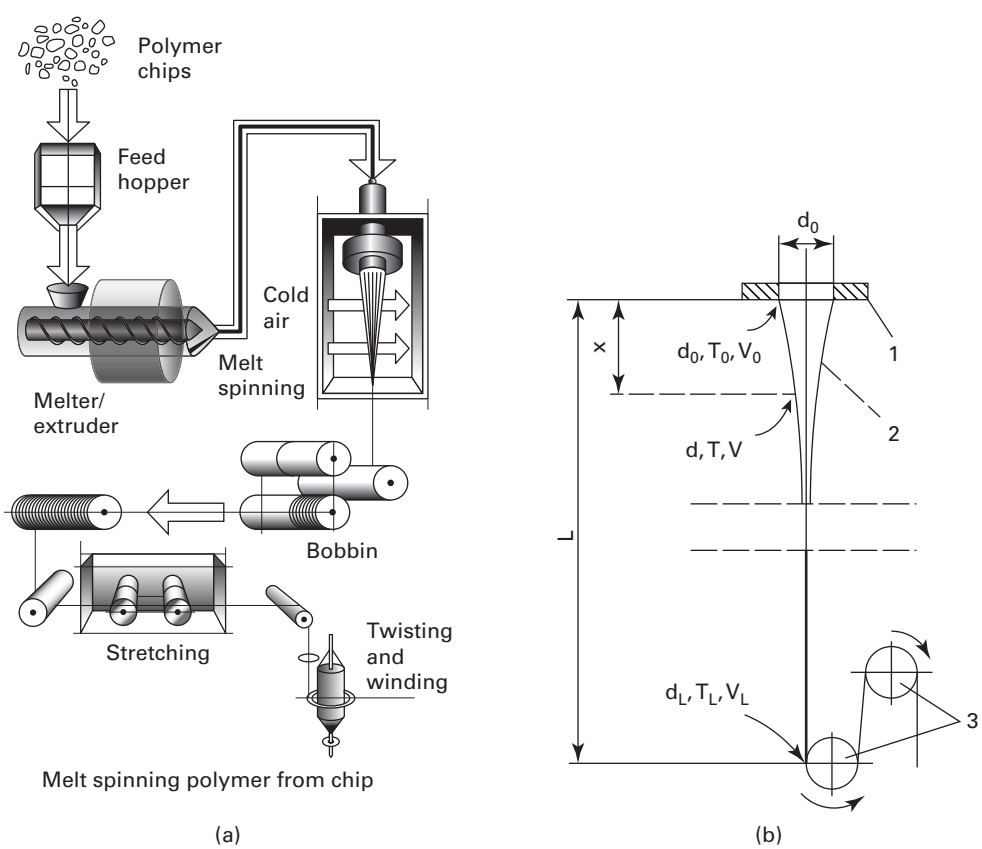

Figure 1.1 (a) Melt spinning (Fiber Source 2013). (b) Schematic of an individual molten threadline in melt spinning process: 1 – spinneret, 2 – molten threadline, which cools down due to convective heat transfer to the surrounding gas and solidifies, 3 – winding bobbin. Ziabicki (1976). Courtesy of John Wiley and Sons.

form in large tows, which are then crimped, heat set and cut into the desired staple lengths. These staple fibers are then blended with other fibers (natural as well as manmade or synthetic fibers) and are formed into a yarn. Most textile yarns are made from blends of various staple fibers; the yarn spinning technology is quite well developed and produces incredibly interesting and desirable textures and properties. Filaments are sometimes textured to form bulk or stretch in post-processing. Many of the facilities have integrated polymer synthesis and fiber formation – that is, the most widespread processes for staple (discontinuous) fiber production couple synthesis and fiber extrusion, and thereby control costs.

Molten threadlines in the melt spinning process are free liquid jets pulled by a winding bobbin to form solidified fibers (Figure 1.1b). These molten threadlines are subjected to several instabilities and perturbation-amplification phenomena, which can make the resulting fibers nonuniform. One of these instabilities, the so-called draw resonance, was discovered in the seminal works of Matovich and Pearson (1969) and Pearson and Matovich (1969), and below we discuss the elementary theory of this phenomenon.

Consider an isothermal straight liquid threadline that is issued from a spinneret hole of radius a_0 with velocity V_0. The longitudinal axis along the threadline axis is denoted x. It is reckoned from the spinneret hole where x = 0. The threadline has a circular cross-section and tapers due to the pulling force transmitted from a winding bobbin located at x = L. The winding velocity imposed by the bobbin on the threadline at x = L is V_1; however, the cross-sectional radius at that point is to be determined.

To formulate the mass and momentum balance and derive the corresponding quasi-one-dimensional equations, we consider an infinitesimally short slice of the threadline of length dx located close to cross-section x. The liquid mass currently contained in this slice is equal to $\rho\pi a^2 dx$, where ρ is the liquid density and a(x,t) is the cross-sectional radius, which depends on x and time t. During the time interval dt, this mass can change, due to the liquid influx through the cross-section x, which is $\rho\pi(a^2V)|_x dt$, and the outflow through the cross-section x+dx, which is $\rho\pi(a^2V)|_{x+dx} dt$, where V(x,t) is the longitudinal velocity in the threadline. The mass balance reads

$$\Delta\left(\rho\pi a^2 dx\right) = \rho\pi\left(a^2V\right)|_x dt - \rho\pi\left(a^2V\right)|_{x+dx} dt \tag{1.1}$$

Using the Taylor series, we see that

$$\left(a^2V\right)|_x - \left(a^2V\right)|_{x+dx} = -\frac{\partial(a^2V)}{\partial x} dx \tag{1.2}$$

and thus Eq. (1.1) reduces to the following differential mass balance, or following the fluid mechanical terminology, continuity equation:

$$\frac{\partial a^2}{\partial t} + \frac{\partial V a^2}{\partial x} = 0 \tag{1.3}$$

In the momentum balance, we neglect inertial forces, surface tension and gravity, and account for only the internal normal stresses acting in the threadline cross-sections and assumed to be dominant. Denote normal stress as σ_{xx}, and thus the corresponding force

acting in cross-section x of the infinitesimal threadline slice under consideration would be $\sigma_{xx}\pi a^2|_x$. Accounting for the force acting at the cross-section x+dx of the slice, we form the momentum balance in the following form

$$\sigma_{xx}\pi a^2|_x - \sigma_{xx}\pi a^2|_{x+dx} = 0 \tag{1.4}$$

which means that

$$\frac{\partial \sigma_{xx} a^2}{\partial x} = 0 \tag{1.5}$$

In the elementary model we are dealing with, we assume that liquid in the threadline is Newtonian fluid and is characterized by a single rheological parameter, viscosity μ (see Loitsyanskii 1966, Landau and Lifshitz 1987, Batchelor 2002). Polymer melts used in melt spinning, as well as polymer solutions used in dry and wet spinning, can hardly be treated as viscous Newtonian liquids, since they develop significant and even dominant elastic stresses in strong elongational flows. Such fluids are viscoelastic. Viscoelasticity is introduced in Chapter 2 and accounted for when considering different types of polymer jet flows and fiber-forming processes relevant to manufacturing of micro- and nanofibers in Chapters 3–5. The simplified rheological model of Newtonian fluids employed here would be directly relevant to the formation of optical fibers (see Sections 6.6 and 6.7 in Chapter 6). Molten glasses are Newtonian liquids, albeit their viscosities are strong functions of temperature. Here, for simplicity, we consider an isothermal case and thus viscosity μ = const.

For the incompressible Newtonian fluids

$$\sigma_{xx} = -p + \tau_{xx} \tag{1.6}$$

$$\sigma_{yy} = -p + \tau_{yy} \tag{1.7}$$

where p is pressure, σ_{yy} is the radial normal stress in the threadline cross-section, and τ_{xx} and τ_{yy} are the normal deviatoric stresses corresponding to σ_{xx} and σ_{yy}, respectively.

Since the outer surface of the threadline can practically always be considered as unloaded because all the tractions imposed by air or surface tension effects are negligibly small in comparison with the inner stresses in the liquid, $\sigma_{yy} = 0$ practically everywhere in the cross-section (Yarin 1993), and thus Eq. (1.7) yields $-p = -\tau_{yy}$. The latter allows transformation of Eq. (1.6) to the following form

$$\sigma_{xx} = \tau_{xx} - \tau_{yy} \tag{1.8}$$

For Newtonian fluids,

$$\tau_{xx} = 2\mu\frac{\partial V}{\partial x}, \quad \tau_{yy} = -\mu\frac{\partial V}{\partial x} \tag{1.9}$$

and thus using Eq. (1.8) we arrive at

$$\sigma_{xx} = 3\mu\frac{\partial V}{\partial x} \tag{1.10}$$

where the factor 3μ is called the Trouton viscosity (Yarin 1993).

Substituting Eq. (1.10) into Eq. (1.5), we transform the momentum balance to the following form

$$\frac{\partial}{\partial x}\left(a^2\frac{\partial V}{\partial x}\right)=0 \tag{1.11}$$

The continuity and momentum balance equations (1.3) and (1.11) form a closed system of the two quasi-one-dimensional equations required to determine two unknown functions, the radius and velocity distributions a(x,t) and V(x,t). These equations represent the simplest version of the quasi-one-dimensional equations of the dynamics of free liquid jets (3.1) and (3.2) discussed in Section 3.1 in Chapter 3.

Render Eqs. (1.3) and (1.11) using the following scales: L for x, $a_0E^{-1/2}$ for a and V_1 for V. Here $E= V_1/V_0$ denotes the draw ratio, which is the governing parameter of this problem. The continuity and momentum balance equations (1.3) and (1.11) in the dimensionless form do not change.

In the case of melt spinning, solutions of the dimensionless system of Eqs. (1.3) and (1.11) are subjected to the following dimensionless boundary conditions:

$$x = 0: a = E^{1/2}, V = E^{-1} \tag{1.12}$$

$$x = 1: V = 1 \tag{1.13}$$

In steady state, the time derivative in Eq. (1.3) vanishes and the steady-state solutions a_s and V_s depend only on x:

$$a_s= E^{(1-x)/2}, V_s= E^{(x-1)} \tag{1.14}$$

Since the draw ratio E is always larger than 1, Eqs. (1.14) describe tapering of the threadline from the cross-sectional radius a_0 to a smaller value $a_1= a_0E^{-1/2}$ at the winding bobbin, whereas velocity is increasing from V_0 to V_1. To form smaller fibers, one is interested in increasing the draw ratio E. This, however, is subject to a severe limitation related to the instability of the steady-state solution (1.14). Indeed, consider small perturbations $\alpha<<1$ and $\beta<<1$ of these solutions, i.e. take

$$a = a_s(x)[1+\alpha(x,t)], V = V_s(x)[1+\beta(x,t)] \tag{1.15}$$

Substituting these distributions into Eqs. (1.3) and (1.11), and linearizing the resulting equations, we arrive at the following system of equations for α and β

$$\frac{\partial\alpha}{\partial t}+V_s\frac{\partial\alpha}{\partial x}+\frac{V_s}{2}\frac{\partial\beta}{\partial x}=0 \tag{1.16}$$

$$2\frac{\partial\alpha}{\partial x}+\frac{\partial\beta}{\partial x}+\frac{1}{\ln E}\frac{\partial^2\beta}{\partial x^2}=0 \tag{1.17}$$

Since the conditions at the spinneret hole and the winding bobbin are assumed to be fixed, the radius and velocity perturbations α and β are subject to the following boundary conditions

$$x = 0: \alpha = 0, \beta = 0 \tag{1.18}$$

$$x = 1: \beta = 0 \tag{1.19}$$

Excluding β from the system of equations (1.16) and (1.17), we reduce it to a single equation for α:

$$\frac{\partial^2 \alpha}{\partial x^2} + E^{(1-x)} \frac{\partial^2 \alpha}{\partial x \partial t} = 0 \tag{1.20}$$

with the corresponding equation relating β to α.

Solving Eq. (1.20) for α, one can find the corresponding β as

$$\beta = -2\alpha + \frac{2E^{(1-x)}}{\ln E} \frac{\partial \alpha}{\partial t} + \frac{2}{\ln E} \frac{\partial \alpha}{\partial x} + \psi(t) \tag{1.21}$$

where ψ (t) is a funtion of t.

The solutions for α and β are subject to the boundary conditions (1.19). As a result, we find the following distribution of the radius perturbation:

$$\alpha = \exp(\gamma t)\, F(x),\ F(x) = \int_0^x \exp\left(\frac{\gamma E^{1-\xi}}{\ln E}\right) d\xi \tag{1.22}$$

where ξ is the dummy variable, and the eigenvalue γ satisfies the following characteristic equation:

$$\gamma = -\frac{F(1)}{\int_0^1 E^{1-\xi} F(\xi) d\xi} \tag{1.23}$$

Solutions γ of Eq. (1.23) are sought on the complex plane.

The investigation of the characteristic equation (1.23) shows that in the range $1 < E < 20.22$ it possesses only the solutions with a negative real part γ_r. Therefore, the perturbations (1.22) decay in time as $\exp(-|\gamma_r|t)$, and the steady-state solution for the molten threadline (1.14) appears to be stable. At $E = 20.22$ the nondecaying small oscillations set in, which corresponds to the solution of Eq. (1.23), $\gamma = 0.693i$, where i is the imaginary unit. Mathematically speaking, this is a classical Hopf bifurcation. At $20.22 < E < 49.98$ the solutions of Eq. (1.23) represent a pair of complex conjugate solutions with a positive real part γ_r. The corresponding linear perturbations grow in time as $\exp(\gamma_r t)$, and the draw resonance sets in (Pearson and Matovich 1969, Pearson 1985). Some of the relevant eigenvalues found from Eq. (1.23) are listed in Table 1.1, where γ_i denotes the imaginary part of γ.

At $E > 20.22$, the instability of the steady-state solution (1.14) results in a bifurcation to a new solution. Under the fixed boundary conditions (1.18) and (1.19), the nonlinear solutions of the continuity and momentum balance equations (1.3) and (1.11) can be found either by the asymptotic method of multiple scales or numerically (Yarin 1993, Yarin *et al*. 1999). The solutions represent the self-sustained oscillations (the so-called limit-cycle solution) illustrated by the numerical results depicted in Figure 1.2. The fiber radius at the winding bobbin a(1,t) becomes a periodic function of time, with the

Table 1.1 Spectrum (1.23) of the linear stability problem. Reprinted with permission from Yarin *et al.* (1999). Copyright 1999, AIP Publishing LLC.

E	γ_r	γ_i
19	–0.0111	0.731
20.22	0	0.693
21	0.00495	0.6723
25	0.01918	0.5869
28	0.0258	0.5369
30	0.029	0.508
35	0.0349	0.4497

amplitude variation in the range 0.5 to 7.5 (see Figure 1.2b). Therefore, formation of uniform fibers at $E > 20.22$ is impossible, and the draw resonance instability severely restricts the increase of the winding speed, the other parameters being fixed.

Donnelly and Weinberger (1975) conducted model experiments with isothermal spinning of Newtonian liquids, intended to verify experimentally the existence of the draw resonance instability. This work represents significant fundamental interest, since it excluded all complicating effects related to the heat transfer at the threadline surface, the elasticity of the polymer melt and solidification. In these experiments a highly viscous silicon oil threadline was drawn by a winding bobbin, from which it was immediately scraped by a doctor blade located close to the bobbin surface. The experiments by Donnelly and Weinberger (1975) showed that the draw resonance sets in as soon as the draw ratio E reaches a value close to 20, in full agreement with the theory. Similar data were obtained by Ishihara and Kase (1976), who employed another liquid, polyethylene terephthalate (PET), with approximately Newtonian behavior. In their case the threadline solidified on contact with the winding bobbin, which was submerged in cold water.

In the general case, perturbations can be also introduced at both ends of molten threadlines due to oscillations of metering pumps, equipment vibratitons and blowing of air for fiber cooling. Then, the question of the threadline sensitivity to the imposed perturbations arises. To illustrate that, consider the case where only perturbations of the initial threadline radius are present, for example, due to the die swell affected by the oscillations of the metering pump. In this case $x = 0$ approximately corresponds to the end of the die swell (the length of the die swell is negligible compared to the length of the threadline). Then, the linearized boundary conditions that replace the boundary conditions (1.18) and (1.19) become

$$x = 0: \ \alpha = \alpha_0 \sin \omega t, \ \beta = 0 \tag{1.24}$$

$$x = 1: \ \beta = 0 \tag{1.25}$$

where α_0 and ω are the dimensionless perturbation amplitude and frequency, respectively.